JCTC Journal of Chemical Theory and Computation

ARTICLE

pubs.acs.org/JCTC

Nature of Chemical Interactions from the Profiles of Electron Delocalization Indices

Marco García-Revilla,[†] Paul L. A. Popelier,[‡] Evelio Francisco,[†] and Ángel Martín Pendás*[,†]

[†]Departamento de Química Física y Analítica, Facultad de Química, Universidad de Oviedo, E-33006-Oviedo, Spain

[‡]Manchester Interdisciplinary Biocentre (MIB), 131 Princess Street, Manchester M1 7DN, United Kingdom and School of Chemistry, University of Manchester, Oxford Road, Manchester M13 9PL, United Kingdom

ABSTRACT: We analyze the behavior of the profiles of delocalization indices (DIs) between relevant pairs of atoms along reaction coordinates for a set of model chemical processes. A relationship between the topology of the DI and the nature of the underlying chemical change is reported. As shown, exponential shapes correspond to the traditional category of repulsive/nonbonded interactions, while sigmoidal profiles signal the formation/breaking of chemical links.

1. INTRODUCTION

The concept of the chemical bond, central to the science of chemistry, is still a matter of lively debate among scholars almost 95 years after Lewis's insights[1] and 50 years after Pauling[2] laid the modern foundations of the field. At the very heart of the problem lies the fact that establishing both when two atoms are bonded or not and when their interaction stabilizes the energy of a molecule are not easy tasks for polyatomics. In fact, they require either techniques to describe atoms in molecules or ways to partition molecular energies into atomic or pair contributions.

In the past few decades, real space theories of the chemical bond have provided an alternative to the molecular orbital (MO)[3] paradigm that has dominated the field. The best known approaches are based on partitioning the real space through the gradient operating on some scalar field endowed with chemical content and are collectively known as Quantum Chemical Topology (QCT).[4,5] Among them, the Quantum Theory of Atoms in Molecules (QTAIM) developed by Bader[6] stands out. In its basic mode of operation, a set of indicators based on reduced density matrices (like the density itself, ρ, the laplacian of the density, $\nabla^2\rho$, the energy density, H, and many others) are obtained at the finite set of distinguished points in space where $\nabla\rho = 0$. These are the critical points (CPs) of the ρ field, and their set of indicators is used to build correlations to chemically important concepts, ranging from bond order and bond type to basicity or reactivity indices.

Recently, one of the best known results of the QTAIM, the identification between bond critical points (BPCs) at stationary molecular configurations[7] and pairs of bonded atoms, has been put into question. In short, BCPs are found where chemists will not place them and vice versa.[8−11] The situation has led to a particularly intense debate regarding the meaning of BCPs in situations that are usually understood as nonbonding (steric, repulsive).[11−16] Examples of this discussion may be found in the recent work of Grimme et al. about the nonexistence of a bonded interaction between the bay moiety hydrogens in phenanthrene[17] and in the study of Henn et al. on the absence of BCPs in $HS(CH)(CH_2)$ and $F(CH_2)_4F$.[18] The debate is in our opinion far from over, and radically opposite interpretations are offered by the supporters of both positions.

Some of us have previously contributed to this discussion by noticing that alternative interpretations to the meaning of BCPs exist.[19] According to our proposal, on the basis of the interacting quantum atoms approach (IQA),[20−23] bond paths signal privileged exchange-correlation (xc) channels between pairs of atoms, thus always providing a locally stabilizing V_{xc} term to the total energy. Since V_{xc} is just one of the terms in the IQA energetic decomposition, this view makes the presence of BCPs fully compatible with global destabilizations. The close relationship of BCPs to the energetic properties of a system connects two paradigmatic views of the chemical bond, the molecular structure due to the topology of $\rho(r)$ and the energetic behavior associated with a bonded system. Such a connection between the structure and the energetics gives an important contribution to the physical meaning of the BCPs and to the partitioning of space provided by the QTAIM.

It is becoming increasingly clear that a common source of this and other criticisms made to QCT resides in its local operating mode. By restricting QCT analyses to examining properties at CPs, we unfortunately subject our description to the lability of these positions in space, which appear and disappear catastrophically upon geometrical rearrangements of the nuclei. Such a sensitivity is absent if QCT focuses on global (i.e., domain-integrated) properties. Global descriptors may involve not only one basin but two, as in the calculation of V_{xc}, or even many, being perfectly suited to identifying relations among atoms. We firmly believe that by using global descriptors, useful insights about the nature of chemical interactions will be found.

In this work, we examine the behavior of one of the simplest two-basin indices, the shared electron delocalization index (SEDI), or delocalization index (DI) for short, and uncover an interesting link between the topology of the DI profile along a reaction coordinate and the nature of the chemical change associated with it. The close algebraic proximity between SEDIs

Received: March 17, 2011
Published: May 13, 2011

(see eq 1 below) and V_{xc}'s[20] pushes us to do so, the latter being an energetic signature of the former. Thus, as the competition of different exchange-correlation energetic contributions between a given atom and its neighbors determines the existence or not of BCPs, DIs may hold interesting information that may be masked in V_{xc} due to the intrinsic dependence on interelectron distances of the latter. As it will show up in the following, the new insights cannot be obtained directly from either V_{xc} or the local values of scalars fields, i.e., densities, laplacians, etc., at BCPs.

Although QCT DI profiles are not new,[24] they have been scarcely used in the literature up to now. For instance, their evolution along reaction paths has been used to study the reactivity and aromaticity in model chemical reactions.[25−29] Similarly, Poater and co-workers[25] have proposed that the changes in the DI are evidence of the reorganization of the electron pairing along the reaction path. Within this interpretation, a DI profile agrees with the predictions of the traditional Lewis model. Another related study was presented by Matito and co-workers,[28] where the behavior of DI and localization index profiles was used to visualize quantitatively the problems of the restricted Hartree−Fock method in reproducing homolitic dissociations. In addition, Ponec and Cooper[26] reported the presence of inflection points in DI profiles for bonded systems, finding no molecule-specific significance to the location of such points. They did not compare bonded and nonbonded systems.

In summary, a literature survey shows that the different shapes of the DI profiles are related to the bonding or nonbonding nature of the interaction that is being followed but that this link has not been explored explicitly up to now. Here, we examine a number of simple, prototypical chemical changes modeled at different levels of theory to substantiate our findings.

2. METHODS, SYSTEMS, AND COMPUTATIONAL DETAILS

The delocalization index between two quantum groups A and B, δ^{AB}, was introduced by Bader and Stephens[30] as a measure of the number of electron pairs delocalized between the groups. Since then, it has been used as a real space measure of the covalent bond order[31] and has been shown to correspond to the real space analogue of the commonly used Wiberg−Mayer bond index.[32,33] δ^{AB} is obtained by a two-electron, two-basin integration of the exchange-correlation density, $\rho_{xc}(1,2) = \rho(1)\,\rho(2) - \rho_2(1,2)$, where ρ_2 is the second order reduced density matrix:

$$\mathrm{DI} = \delta^{AB} = 2\int_A \mathrm{d}1 \int_B \mathrm{d}2\, \rho_{xc}(1,2) \qquad (1)$$

In the case of single determinant (SD) wave functions, ρ_{xc} may be factorized in terms of the nondiagonal first order density matrix:

$$\begin{aligned}\rho_{xc}(1,2) &= \rho(1;2)\,\rho(2;1)\\ &= \sum_{i,j} \phi_i(1)\,\phi_j(1)\,\phi_i(2)\,\phi_j(2)\end{aligned} \qquad (2)$$

where the sums run over all of the occupied spin orbitals ϕ. In this way, the DI is written in terms of domain-restricted overlap integrals, or atomic overlap matrices (AOM), $\delta^{AB} = 2\Sigma_{i,j} S^A_{ij} S^B_{ij}$. This expression has many times been taken as the definition of the DI but is rigorously valid only in the Hartree−Fock approximation. If correlation is deemed important, as in many of the cases we are going to present, then the full four-index representation of the second order density has to be used, and more cumbersome expressions appear. Nevertheless, the DI may always be written as a linear combination of AOM elements, and thus no true 6D integrations are actually needed for its evaluation. With this 3D factorization, the computational complexity of obtaining DIs is not larger than that in the usual 3D integrations of the QTAIM. This is no longer true for other two-electron indices like V_{xc}. As a consequence, DIs are among the only two-electron properties that are commonly obtained in standard QTAIM packages, at least for SD wave functions. We have developed efficient methods to compute DIs in the case of multideterminant expansions of Ψ,[34] and expressions based on density matrix functional theory approximations to ρ_{xc} have also been developed.[35,36]

A connection between the DI and the fluctuation of the basin populations exists.[30,37−39] It may be shown that the covariance of the joint probability distribution for the number of electrons in the basins A and B is given by the DI:

$$\delta^{AB} = -2\mathrm{cov}(n_A, n_B) = -2[\langle n_A n_B\rangle - \langle n_A\rangle\langle n_B\rangle] \qquad (3)$$

where $\langle n_A n_B\rangle = \Sigma_{n_A,n_B} n_A n_B p(n_A,n_B)$ and $\langle n_A\rangle = \Sigma_{n_A} n_A p(n_A)$. In these expressions, $p(n_A)$ and $p(n_A,n_B)$ are electron number distribution functions (EDFs). The first provides the probabilities of observing an exactly integer number of electrons n_A in basin A and the second, the joint probability of finding n_A electrons in basin A and n_B electrons in basin B. Since there are now efficient methods to construct such EDFs,[40−42] an interesting interpretation is emerging in which chemical bonding is interpreted in terms of the fluctuation in the number of electrons associated with quantum atoms. In a diatomic, for instance, the constancy of the total number of electrons $N = n_A + n_B$ forces any change in the population of one basin to be accompanied by a symmetric (and opposite in sign) change in the other. The DI (minus covariance) in such a case is a necessarily positive quantity, a property that does not necessarily hold in general polyatomic systems. DIs are (contrarily to other atomic expectation values, like the kinetic energy) perfectly defined for any pair of nonoverlapping regions of the 3D space. They will be positive-definite if the integrand is positive-definite. This is not true, for ρ_{xc} may take negative values whenever the Coulomb correlation contribution dominates over the Fermi one. This means that we may in principle find two regions of space with negative ρ_{xc} that will give a negative DI. What is necessarily true is that the sum of all delocalization and localization values, i.e., the integral over the full 6D space of ρ_{xc}, must be positive and equal to N, the number of electrons in the molecule. We think that it is very unlikely that a negative DI will show up between two entire atomic regions. This would mean that the Coulomb correlation overcomes the Fermi contribution over large regions, something not very plausible, but not impossible. In any case, positive values will arise whenever the populations of two basins are negatively correlated. In other words, whenever there is a direct physical exchange of electrons between the basins. Using this kind of insight, we have shown[41] how the bond order may be interpreted in terms of the number of electrons of one basin that may be exchanged with the other, providing an intuitive view of well-known traditional concepts.

Following some reported observations based on the shape of both Wiberg indices[43,44] and QCT DIs,[24,45] we have selected a number of simple chemical processes and studied the behavior of DIs along their intrinsic reaction coordinates (IRC). The use of IRCs allows us to map the complex geometric rearrangements following a reaction onto a unique scalar parameter. The processes examined include dissociations, atomic exchanges,

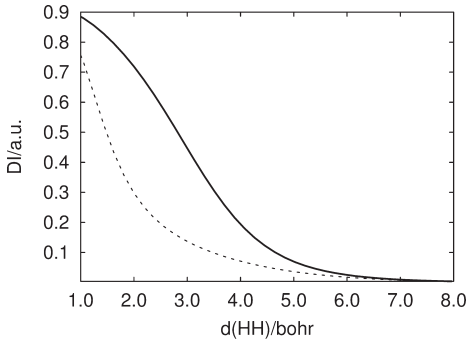

Figure 1. Delocalization index versus HH distance for the dissociation of singlet (full line) and triplet (dotted line) H_2.

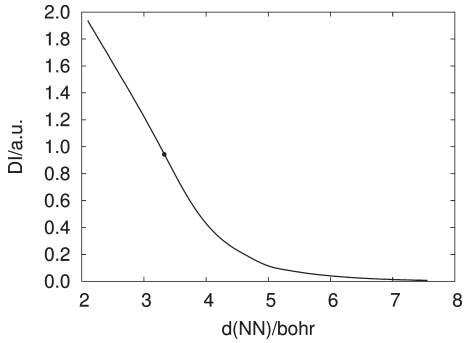

Figure 2. Delocalization index versus NN distance for the dissociation of N_2. The inflection point has been highlighted.

migrations, intramolecular rearrangements, and a few of the controversial systems commented on before. Some of these processes are well represented at the Hartree−Fock (HF) level, and since our purpose here is not quantitative, we present such low level calculations. Other dissociations, particularly open-shell ones, cannot be adequately described if correlation is not taken into account. In such cases, appropriate multideterminant calculations will be reported, either at the CAS or CISD level.

All electronic structure calculations, including optimizations, transition state (TS) searches, and constrained optimizations, have been performed with the GAMESS[46] code using the 6-311++G(d,p) basis set. DIs have been obtained with our PROMOLDEN code.

3. RESULTS

We will begin our discussion by examining the dissociation of simple bonded and nonbonded diatomics, starting with H_2. We have previously reported[47] an EDF/IQA analysis in this system to which the reader is referred for further insights, but no explicit account of the behavior of DIs was given there.

3.1. The Dissociation of Diatomics. We have examined the formation and breaking of several homo- and heteronuclear diatomics. Here, we report on the dissociation of H_2, N_2, He_2, Ar_2, and LiH.

The breaking of the first molecule is the paradigm of an open-shell process, so we will use a CAS[2,2] description. It provides the simplest wave function that fully describes the process. Figure 1 shows the variation of DI(HH) with the internuclear separation for both the $X^1\Sigma_g^+$ and $b^3\Sigma_u^+$ states. The optimization of the former gives rise to the ground state of H_2 at an internuclear distance of about d = 1.4 bohr, while the latter is a repulsive state. The effect of correlation in the singlet is essential, since a SD description provides DI = 1 at any internuclear distance. This may be interpreted as a result of the statistical independence of α and β electrons at the HF level that leads, through eq 3, to a binomial distribution of the electron populations in both basins. Thus, the probabilities of finding simultaneously n_A and n_B electrons in each basin becomes $p(2,0) = p(0,2) = 0.25$ and $p(1,1) = 0.5$.[47] Introduction of α,β correlation partially localizes both electrons, and $p(1,1)$ increases so that DI = 2 − $2p(1,1)$ decreases. The two α electrons are always correlated in the triplet state, even in a SD description.

The DI profiles for the H_2 dissociation of the singlet and triplet states are shown in Figure 1, the singlet profile is similar to that reported by Matito and co-workers.[28] As we can observe, the topology of the DI profiles is qualitatively different in both cases, the singlet displaying a clearly developed inflection point that is absent in the triplet. As we will illustrate throughout this work, this property seems rather general. Another interesting aspect is the position of the inflection point. A polynomial fit determines it occurring at $d \approx 2.90 \pm 0.1$ bohr, where DI = 0.5 ± 0.1.

There are several possible interpretations for this DI = 1/2 value, and the simplest one relates it to a half-formed (or broken) bond. In the independent electron approximation, a full covalent (2*c*,2*e*) symmetric link with DI = 1 is the result of two completely delocalized electrons, each of them displaying a probability 1/2 of being found in any of the atoms. Similarly, two isolated electrons, one found exclusively in basin *A* and the other in basin *B*, are the signature of a noninteracting system. A 50/50 statistical mixture of both descriptions gives rise to the EDF $p(2,0) = p(0,2) = 0.125$, $p(1,1) = 0.75$, which is that found at DI = 0.5. Finally, the sigmoidal shape of the DI profile in the singlet curve points toward a kind of cooperative transition in which the internuclear distance plays the role of an order parameter. It is the presence or absence of this transition that seems to distinguish the nature of the process.

The H_2 example shows very clearly why the information introduced by DI profiles is new, not contained in other quantities explored up to now. First, it is not contained in the variation of V_{xc}'s with interbasin distance. For both the singlet and triplet states, V_{xc}^{AB} decreases exponentially in H_2. It is also not contained in local scalars computed at BCPs. Given that there is no V_{xc} competition in this diatomic system, a BCP is present at any internuclear separation. The density, for instance, decays exponentially, in both states, although it is larger in the singlet. Similarly, the laplacian becomes negative for both the singlet and the triplet at distances smaller than a given (of course, different) threshold value. The DI profiles are, nevertheless, qualitatively different.

We have also studied the dissociation of the dinitrogen molecule at the CAS[10,8] level, with r_e = 2.10 bohr, and our results are shown in Figure 2. The sigmoidal shape is qualitatively similar to the one displayed in Figure 1. The inflection point is located at $d \approx 3.3 \pm 0.1$ bohr, where DI = 0.9 ± 0.1. Such a behavior is thus related with the breaking of the covalent interaction along the process, as was pointed out in the case of H_2 dissociation. Notice how the value of the DI at the inflection point is again located at about half the DI value attained at the equilibrium geometry.

Other simple dissociations have also been considered. In bonded homodiatomics, the results are completely equivalent to those found in H_2 and N_2 and do not deserve further

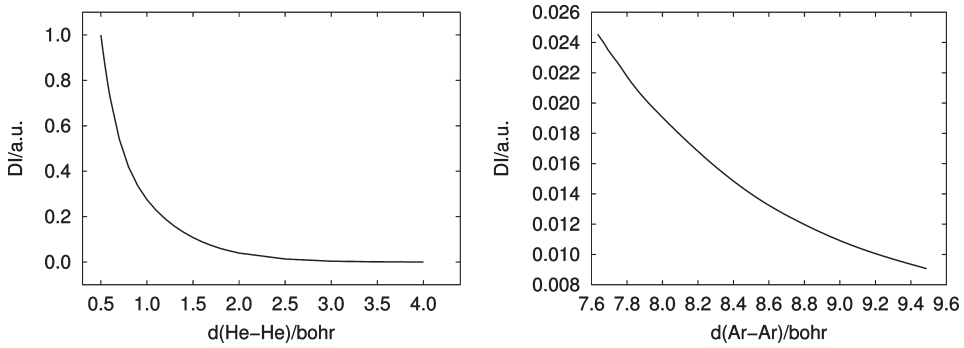

Figure 3. Delocalization index versus internuclear distance for the dissociation of ground state He_2 and Ar_2 molecules.

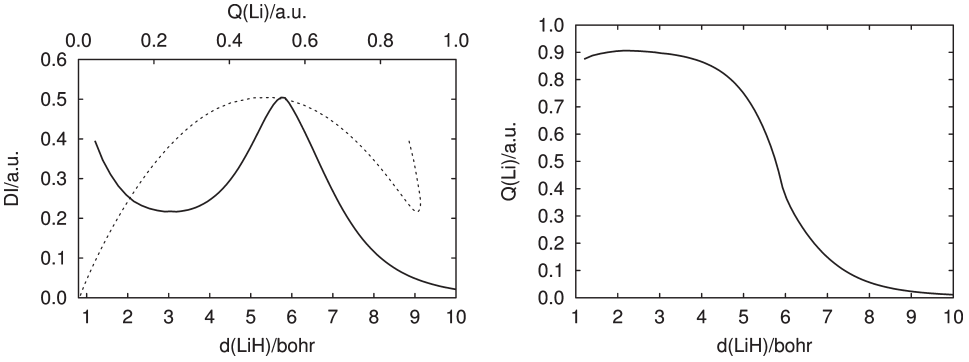

Figure 4. DI profiles in the dissociation of LiH at the CAS[2,2] level. (Left) DI versus the LiH internuclear distance (full line). The same DI profile is also shown versus the topological charge of Li (dotted line). Charge values less than 0.5 are related to the covalent regime, and values close to 1.0 are located in the ionic regime. (Right) Sigmoidal shape of the variation of the topological charge of Li versus the internuclear separation.

comment. More interesting is an examination of traditionally nonbonded interactions. Figure 3 contains the DI profiles for the dissociation of He_2 and Ar_2, calculated at the CISD. In both cases, the results are qualitatively similar, and the DI grows more or less exponentially as the internuclear distance decreases. Notice how the nonbonded/repulsive character of the interactions is mapped onto a monotonous profile both for an excited state of a bound system (triplet H_2) and for the ground states of unbound diatomics.

Dissociation processes in heterodiatomics are more interesting, particularly when avoided crossings occur. Figure 4 shows the DI for the dissociation of LiH in a CAS[2,2] calculation. Similar results have already been reported.[26,29,45] An avoided crossing between the ionic and neutral states is found at about d = 5.5 bohr, closely corresponding to the maximum in the DI profile and to the region where DI = 0.5.

The basic characteristics of this shape may be easily modeled as a unidirectional charge transfer (CT) of one electron from H to Li. Actually, from d = 3 to d = 10 bohr, the EDF of the system is reproduced to better than 1% by just two contributions, $p(2,2)$ and $p(3,1)$, where the first figure corresponds to the number of electrons in the Li basin. Were the process a linear transfer of the electron from H to Li, going from $p(2,2) = 1$ (and $p(3,1) = 0$) to $p(2,2) = 0$, the DI would show an inverted parabolic shape starting and ending at DI = 0, and peaking at DI = 0.5 when half an electron had been transferred. The results shown in the figure display very good quadratic behavior, except in the vicinity of the equilibrium geometry.

This tells us that the nonparabolic variation of the DI with internuclear distance is due to the nonlinear character of charge transfer, which is depicted on the right side of Figure 4. The variation of CT with d is again sigmoidal,[45] with an inflection point at about the avoided crossing (or DI maximum). It is also worth noticing that the equilibrium geometry, $d \approx 3.0$ bohr, is close to the DI minimum shown in the figure. At smaller distances, another delocalization channel appears: $p(1,3)$ starts to increase, and so does the DI in a nonbonding manner. DI profiles with a local maximum thus indicate charge transfers or ionic interactions.

The sigmoidal variation of Q(Li) with distance reinforces the idea that cooperative phenomena underlie bonding landscapes. This may be worked out in slightly more detail by noticing that general $(2c,2e)$ symmetric delocalizations, as well as $(2c,1e)$ CTs, may be modeled with a single electron transfer coordinate $t \in [0,1]$ that measures the degree of delocalization or CT, respectively. In a homodiatomic case like H_2, the two electron EDF may always be written as the direct product of two symmetric one-electron distributions: for the first electron, $p(1,0) = t/2$ and $p(0,1) = 1 - t/2$; for the second, $p(1,0) = 1 - t/2$ and $p(0,1) = t/2$. Notice that t values $\in [1,2]$ simply correspond to a basin exchange and need not be considered. With this model, $\delta^{AB} = t$, and the transfer parameter behaves sigmoidally. In the ionic case, the parameter is just the probability that the transferred electron lies in the final basin, so $t = p(1,0) = Q(\mathrm{Li})$ is sigmoidal. In both cases, the inflection point of the t curves is very close to $t = 1/2$. Further work related to the possible universal behavior of the t versus distance curve clearly needs to be done.

3.2. Other Dissociations. We have examined other bonded and nonbonded dissociations. The first category is represented

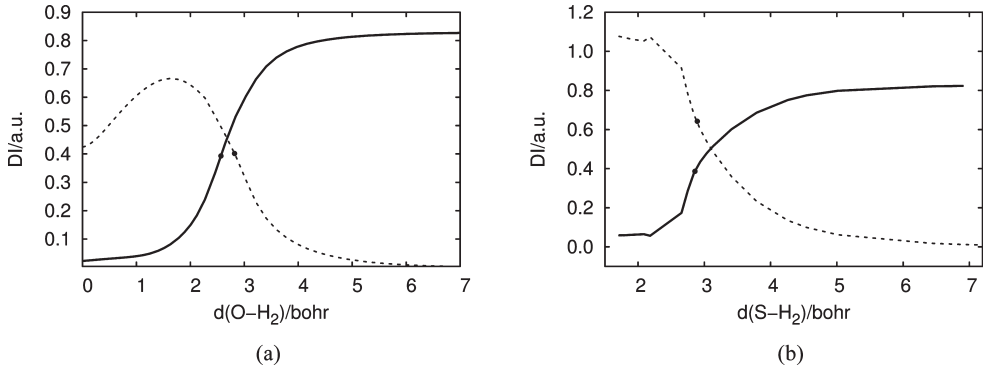

Figure 5. DI profiles for the $H_2X \rightleftharpoons H_2 + X$ dissociations: H_2O (a) and H_2S (b). Both δ^{HX} (dotted lines) and δ^{HH} (full lines) are shown. The inflection points of the curves are marked with filled circles, and d is the perpendicular distance from the X atom to the H_2 axis.

by the approach of X = O and S atoms in their ^1D state to a ground state H_2 molecule to form a H_2X molecule. These are well studied processes that may also be described as H_2 subtractions from H_2X systems, which are recognized as emblematic examples of the change in connectivity along a chemical reaction in the QTAIM.[6] The C_{2v} symmetry has been maintained at all points, such that the X atom evolves along a line perpendicular to the H_2 axis passing through its center. Let us call d the perpendicular distance between X and the H−H axis.

The case of H_2O was used in our previous study on the reinterpretation of bond paths as privileged exchange channels.[19] There, the behavior of V_{xc} was examined, while we focus here on the relevant DIs. To follow this dissociation channel, a size-consistent CAS[6,8] level has been selected. At the H_2X equilibrium configurations, d = 1.138 and 1.710 bohr in water and H_2S, respectively.

Figure 5 displays our computed DI profiles using d as a reaction coordinate. A simple consideration of their shape allows us to neatly classify the underlying chemistry. For instance, in the H_2O case, we distinguish a covalent one-parameter dissociation for the H−H pair as d decreases coupled to a mixture of covalent association and charge transfer processes for O−H. We identify the presence of a mixture by the peak DI value, $\delta^{OH} \approx 0.65$. Any value of DI larger than 0.5 cannot be attained via a one-electron transfer. It is possible to model the shapes of these DIs with two parameters, and on doing so one may justify the deviation in the position of the inflection point (or the DI maximum) with respect to the one parameter ideal values shown in the last subsection. However, since our purpose is to qualitatively show the link between the DI shape and the nature of an interaction, we will not pursue this here. The situation in H_2S is similar, although the HS covalency is considerably larger in this case, and the charge transfer maximum is barely visible. The H_2S dissociation was calculated at the CAS[6,8] level of theory.

At the beginning of the reaction the sulfur shares a bit more than one electron pair with each hydrogen, and at the end the hydrogens share a correlated value of about 0.8. A fitted polynomial locates the inflection point at $d \approx 2.85 \pm 0.01$ bohr with DI $\approx 0.40 \pm 0.01$ for the H−H interaction and at $d \approx 2.89 \pm 0.01$ bohr with DI $\approx 0.64 \pm 0.01$ for the H−S interaction. As in the H_2O case, these values are related to the mixing of covalent and ionic terms.

Finally, let us briefly show a repulsive/nonbonded polyatomic case. Figure 6 displays the evolution of the DI between the two clashing hydrogens in the head to head approach (or dissociation) of two methane molecules $H_3C{-}H\cdots H{-}CH_3$ such that the C_{3v} axis is preserved. This is a closed-shell

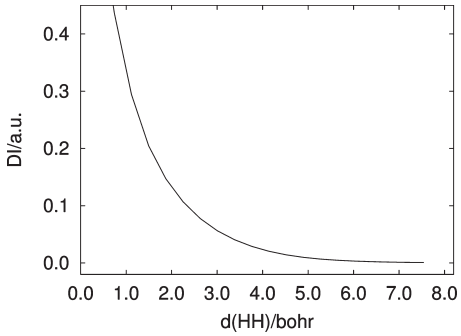

Figure 6. DI profile for the $H_3C{-}H\cdots H{-}CH_3$ process examined in this work. d is the distance between the head-on approaching hydrogens.

interaction that is qualitatively well described at the RHF level. The distance between the approaching hydrogens at the equilibrium geometry is about 7.92 bohr. As seen, there is no hint of inflection point, and the delocalization index falls off exponentially as the two hydrogens separate, being practically zero at the equilibrium geometry.

3.3. Atomic (or Bond) Exchanges. Processes in which bonds are broken at the expense of the formation of others are also interesting and worth studying. The simplest one is the linear exchange of H with a H_2 (or D2) molecule, H1 + H2−H3 → H1−H2 + H3, which is correctly described by even a single-determinant high-spin wave function. This type of change has been studied by Yamasaki and Goddard[43,44] using the equivalent to DIs in Fock space with Mulliken and Löwdin charge operators. Their correlation analysis for chemical bonds (CACB) technique gave rise to fairly similar results to those found here. Figure 7a shows the H2−H3 and H1−H2 DIs along the IRC. Since the reaction is completely symmetric, we find a concerted mechanism in which one bond is being formed while the other is being broken. Correspondingly, the DIs of both pairs are sigmoidal and symmetric, with their inflection points coinciding exactly with the transition state at IRC = 0.

Since the hydrogen exchange may be understood as a bond exchange process, it is also interesting to examine the behavior of the sum of both DIs. Figure 7 shows how, apart from a small rise in the transition state region, the sum turns out to be essentially constant. This supports[44] the use of the sum of the DIs involving a given atom A, $\Sigma_X \delta^{AX}$, as a measure of its free valence or bonding capacity. The wave functions were obtained with the ROHF level of theory.

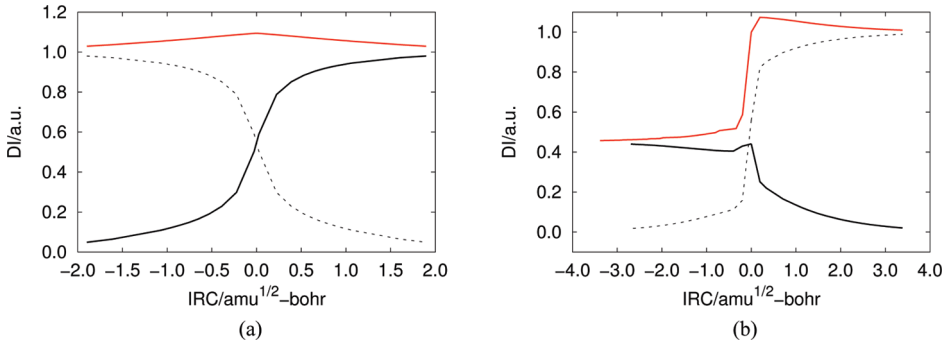

Figure 7. DI profiles for hydrogen exchange reactions. Left, H1 + H2−H3 → H1−H2 + H3. Dashed and full lines are used for the H2−H3 and H1−H2 pairs, respectively. Right, H1 + F−H2 → H1−H2 + F. Dashed and full lines are used for the HH and the HF pairs. For both systems, the sum of the DIs is shown in red.

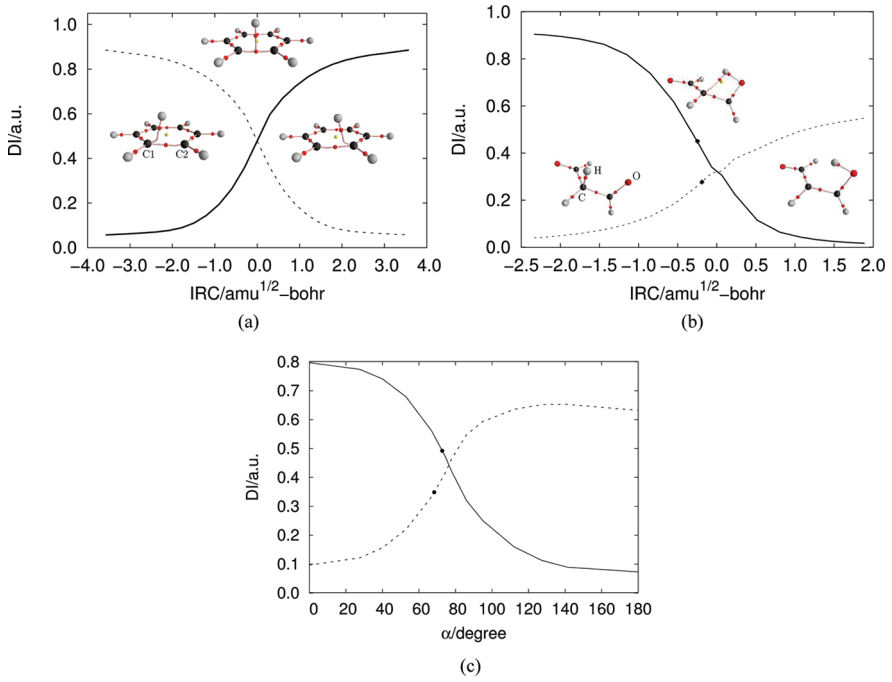

Figure 8. DI profiles for the intramolecular migrations studied in this work. In part a, we show the symmetric DIs for the HC_1 and HC_2 pairs in the benzenium cation 1−2 hydrogen migration. In part b, the malonaldehyde keto−enol tautomerism is examined, with the HO and HC pairs indicated by a dashed and full line, respectively. In part c, we show the HCN to CNH isomerization, using as IRC the angle α between the H to center-of-mass line and the CN internuclear axis. The HC and HN pairs are marked with dashed and full lines, respectively.

A more complex, interesting case is the fluorine−hydrogen exchange H1 + F−H2 → H1−H2 + F presented in Figure 7b, also at the ROHF level. The H1−H2 DI displays the same shape shown in the H + H2 system, while the H1−F does not. As H1 approaches the F−H2 molecule, the F−H_2 DI starts to decrease slowly from its leftmost IRC value, 0.45. This small value indicates a rather large ground state ionicity, and the topological net charges at this stage are $q(H2) = 0.743$, $q(H1) = 0.008$, and $q(F) = -0.750$. As the reaction progresses, δ^{FH2} displays a shallow minimum around −0.5 IRC, and an inverted parabolic shape peaking at about the TS followed by a more or less exponential decrease toward the F dissociation. Notice how the region around the TS coincides with the relevant chemical changes, in agreement with intuition. At the peak of the F−H2 DI curve, $q(H1) = 0.120$, $q(H2) = 0.008$, and $q(F) = -0.128$, and we clearly see the transition between the starting and the final bonding situation. We may therefore follow the chemical changes easily from reading the DI figure: a covalent HH link is formed at the expense of the HF bond in the first stage. This is followed by a charge transfer process in the vicinity of the TS. Once this process is completed, the fluorine is expelled as the HH link consolidates.

As in the previous case, we have also considered the sum of both DIs, which is well described as a sudden jump between two rather well-defined values. If this jump is washed out from Figure 7b, the behavior of the DI sum is pretty similar to that in the H + H_2 case, being constant apart from a small increase in the TS region. The jump is to be associated with the sudden availability of an electron for the construction of a covalent bond H−H, and thus to the transfer of that electron from the F basin toward the H2 one.

3.4. Migrations. Intramolecular migrations are good examples of coupled formation and breaking of chemical bonds. In

dx.doi.org/10.1021/ct2001842 |J. Chem. Theory Comput. 2011, 7, 1704–1711

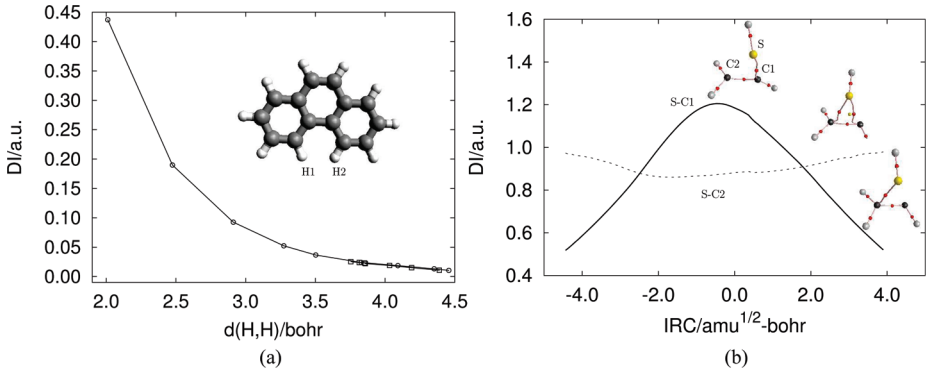

Figure 9. (a) DI evolution of the symmetric (open circles) and asymmetric (open squares) modes for the H1−H2 interaction in the bay moiety of phenanthrene. (b) DI profile and structural change graphs during the CH rotation in $CHCH_2SH$. The ring structure ephemerally exists close to the rightmost line crossing.

topological terms, they are accompanied by the transformation of bond critical points using either the conflict or the bifurcation mechanisms, using the terminology of catastrophe theory as applied to chemical structural change.[6] We have studied three DI profiles of prototropic migrations: the 1−2 intramolecular hydrogen migration of the benzenium cation,[48] the keto−enol tautomerism in malonaldehyde,[49] and the H−C≡N ⇌ H−N≡C isomerization.

Figure 8a contains the relevant DIs in the 1−2 hydrogen migration process in the benzenium cation, calculated at the CAS[6,6] level. The graph shows the DI of the migrating hydrogen with the two carbons directly involved in the reaction. As in the H + H2 case, the reaction is symmetric, and the inflection point is located exactly at the TS. At the beginning of the reaction, the DI between the migrating H and the C1 is 0.9 and decreases as the hydrogen moves to the TS. This process is synchronically coupled to the increase in the HC2 DI and shows that our expectations based on the argument explored in this work are again fulfilled. At the inflection point, DI ≈ 0.5, and we have a rather standard covalent-to-covalent transition that may be modeled uniparametrically.

We have obtained the profiles for the malonaldehyde keto−enol tautomerism at the RHF level and plotted them in Figure 8b. As shown, the behavior is basically the same as in the benzenium cation case, the differences associated to the change in ionicity, much larger in the final situation where a HO link is present than in the initial one, which is characterized by a rather covalent HC bond. This forcibly leads to a rather large H−C DI of about 0.9, to be compared with its H−O equivalent, about 0.5. The inflection points are placed to the left of the TS. It is to be noticed that in both cases, the inflection points are located at about half the total height of the sigmoids, and that the HO curve displays it at a very small DI value, about 0.25. This half-width position is quite general in all of the cases examined.

Finally, the HCN isomerization is examined in Figure 8c, again at the RHF level. The behavior is similar, but this time we may appreciate a shallow maximum in the HN DI that offers a clear indication of partial charge transfer.

3.5. Controversial Cases. In order to include systems where bond paths cause controversy, two systems have been studied: the normal modes assigned to the stretching of the HC bonds for the hydrogen atoms located in the bay moiety of the phenanthrene molecule and the rotation of the CH fragment in $CHCH_2SH$. The first system has been used by Grimme et al.[17] to purportedly show that both theoretical models and the spectroscopic assignment of the experimental IR stretching modes are in agreement with a repulsive H1H2 interaction in the bay moiety of phenanthrene. Thus, the role of the BCP that is found between both hydrogens in QTAIM analyses is put into question. The second has been presented by Henn et al.[18] as an example of a molecule where a chemical bond is absent between two atoms (the SC1 pair), while other theoretical tools, like the natural bond orbital formalism of Weinhold and Landis,[50] state that it is present. We have computed DI profiles in both systems at the RHF level.

The DI between the H1 and H2 atoms in phenanthrene at selected geometries has been constructed following the eigenvectors of their HC stretching normal modes. Figure 9a shows its evolution in the symmetric and asymmetric cases. The distance between the bay moiety hydrogens at the equilibrium geometry is about 3.83 bohr. According to the experience gained with the previous examples, the absence of inflection points along the symmetric-mode coordinate is compatible with a nonbonded/repulsive process, as observed throughout this work. Since the H1−H2 distance hardly varies along the asymmetric motion, the DI evolution in this normal mode is difficult to interpret and will not be pursued anymore.

In our second example, a bond path is expected between the sulfur and the C1 carbon, but topological analyses reported at several levels of theory[18] do not find it at the equilibrium geometry. To further investigate this problem, we have computed the TS and IRC along the rotation of the C1H between two quasi-degenerate conformers that differ in the position of the C1 hydrogen. In this transition, see Figure 9b, the system evolves between the conformers by passing through two three-centered ring regions where SC1 BCPs exist. These BCPs are broken through a bifurcation mechanism. Along the process, δ^{SC2} oscillates in a small window with a width equal to 0.1 around a clearly covalent value of about 0.9, but the SC1 DI widely changes between 0.5 and more than 1.2. According to the insights developed in this work, it is rather clear that the SC1 interaction is basically electrostatic in both conformers and that only in configurations where the hydrogen atom linked to the C1 carbon is close to coplanar with the SC1C2 plane do we find delocalization indices compatible with a SC1 bond.

4. CONCLUDING REMARKS

In this work, we have shown compelling evidence that the topology of the profiles of QTAIM delocalization indices in simple chemical processes keeps information about the nature of

the chemical changes that are taking place. Three basic modes have been uncovered. For repulsive/nonbonded cases, the evolution of the DI turns out to be exponential. In bonded interactions, two extreme cases appear. In the first, associated to covalent or shared interactions, the DI shape is sigmoidal. Contrarily, a bell-like profile is found when charge transfers are involved. We have also shown how one-parameter models for the ideal electron distribution functions in covalent and ionic cases are compatible with these findings if the charge transfer parameter evolves sigmoidally with the reaction coordinate. We think that this points to cooperative phenomena as major players in the formation or breaking of chemical bonds. Interestingly, the information provided by DI profiles seems not to be present in the variation of local scalar fields at bond critical points.

The behavior here uncovered seems of fairly general validity. Dissociations, both in diatomics and polyatomics, bond exchanges, and inter- and intramolecular migrations seem to follow it, and the qualitative pattern is quite independent of the theoretical level used in the computations. Since calculating DIs is considerably cheaper than performing a full QTAIM energy partitioning analysis, the use of the correlations proposed here may help in discerning the nature of chemical interactions in controversial cases, as we have tried to show by examining a few recent examples. We want to stress, however, that as with many other findings in real space theories of chemical bonding, the relationships here explored are empirical and that we are not aware of any formal justification of them. Further work in this direction is welcome.

AUTHOR INFORMATION

Corresponding Author

*E-mail: angel@fluor.quimica.uniovi.es.

ACKNOWLEDGMENT

The authors are thankful for the financial support from the Spanish MICINN, Project No. CTQ2009-08376, the European Union FEDER funds, the MALTA-Consolider program (CSD2007-00045), and FICyT Project No. IB09-019.

REFERENCES

(1) Lewis, G. N. *J. Am. Chem. Soc.* **1916**, *38*, 762.
(2) Pauling, L. *The Nature of the Chemical Bond*, 3rd ed.; Cornell Univ. Press.: Ithaca, NY, 1960.
(3) Gimarc, B. M. *Molecular structure and bonding. The qualitative molecular orbital approach*; Academic Press: New York, 1979.
(4) Popelier, P. L. A.; Brémond, E. A. G. *Int. J. Quantum Chem.* **2009**, *109*, 2542.
(5) Popelier, P. L. A.; Aicken, F. M. *Chem. Phys. Chem.* **2003**, *4*, 824.
(6) Bader, R. F. W. *Atoms in Molecules*; Oxford University Press: NY, 1990.
(7) Bader, R. F. W. *J. Phys. Chem. A* **1998**, *102*, 7314.
(8) Cioslowski, J.; Mixon, S. T *J. Am. Chem. Soc.* **1992**, *114*, 4382.
(9) Haaland, A.; Shorokhov, D. J.; Tverdova, N. V *Chem.—Eur. J.* **2004**, *10*, 4416.
(10) Farrugia, L. J.; Evans, C.; Tegel, M. *J. Phys. Chem. A* **2006**, *110*, 7952.
(11) Haaland, A.; Shorokhov, D. J.; Tverdova, N. V. *Chem.—Eur. J.* **2004**, *10*, 4416.
(12) Bader, R. F. W.; Fang, D.-C. *J. Chem. Theory Comput.* **2005**, *1*, 403.
(13) Poater, J.; Solà, M.; Bickelhaupt, F. M. *Chem.—Eur. J.* **2006**, *12*, 2889.
(14) Poater, J.; Solà, M.; Bickelhaupt, F. M. *Chem.—Eur. J.* **2006**, *12*, 2902.
(15) Bader, R. F. W. *Chem.—Eur. J.* **2006**, *12*, 2902.
(16) Poater, J.; Visser, R.; Solà, M.; Bickelhaupt, F. M. *J. Org. Chem.* **2007**, *72*, 1134.
(17) Grimme, S.; Mück-Lichtenfeld, C.; Erker, G.; Kehr, G.; Wang, H.; Beckers, H.; Willner, H. *Angew. Chem., Int. Ed.* **2009**, *48*, 2592.
(18) Henn, J.; Leusser, D.; Stalke, D. *J. Comput. Chem.* **2007**, *28*, 2317.
(19) Martín Pendás, A.; Francisco, E.; Blanco, M. A.; Gatti, C. *Chem.—Eur. J.* **2007**, *13*, 9362.
(20) Francisco, E.; Martín Pendás, A.; Blanco, M. A. *J. Chem. Theory Comput.* **2006**, *2*, 90.
(21) Martín Pendás, A.; Blanco, M. A.; Francisco, E. *J. Comput. Chem.* **2007**, *28*, 161.
(22) Blanco, M. A.; Martín Pendás, A.; Francisco, E. *J. Chem. Theory Comput.* **2005**, *1*, 1096.
(23) Francisco, E.; Martín Pendás, A.; Blanco, M. A. *J. Chem. Theory Comput.* **2006**, *2*, 90.
(24) Ángyán, J. G.; Loos, M.; Mayer, I. *J. Phys. Chem.* **1994**, *98*, 5244.
(25) Poater, J.; Solà, M; Duran, M.; Fradera, X. *J. Phys. Chem.* **2001**, *105*, 2052.
(26) Ponec, R.; Cooper, D. L. *THEOCHEM* **2005**, *727*, 133.
(27) Matito, E.; Poater, J.; Duran, M.; Solà, M. *THEOCHEM* **2005**, *727*, 165.
(28) Matito, E.; Duran, M.; Solà, M. *J. Chem. Educ.* **2006**, *83*, 1243.
(29) Matito, E.; Solà, M.; Salvador, P.; Duran, M. *Faraday Discuss.* **2007**, *135*, 325.
(30) Bader, R. F. W.; Stephens, M. E. *J. Am. Chem. Soc.* **1975**, *97*, 7391.
(31) Fradera, X.; Austen, M. A.; Bader, R. F. W. *J. Phys. Chem. A* **1999**, *103*, 304.
(32) Wiberg, K. B. *Tetrahedron* **1968**, *24*, 1083.
(33) Mayer, I. *Chem. Phys. Lett.* **1983**, *97*, 270.
(34) Martín Pendás, A.; Francisco, E.; Blanco, M. A. *J. Comput. Chem.* **2004**, *26*, 344.
(35) Fulton, R. L. *J. Phys. Chem.* **1993**, *97*, 7516.
(36) Wang, Y. G.; Werstiuk, N. H. *J. Comput. Chem.* **2003**, *24*, 379.
(37) Bader, R. F. W.; Stephens, M. E. *Chem. Phys. Lett.* **1974**, *26*, 445.
(38) Chamorro, E.; Fuentealba, P.; Savin, A. *Electron J. Comp. Chem.* **2003**, *24*, 496.
(39) Savin, A. Probability Distributions and Valence Shells in Atoms. In *Reviews of Modern Quantum Chemistry*; Sen, K. D., Ed.; World Scientific Publishing: Singapore, 2002; Vol. 1, pp 43−62.
(40) Francisco, E.; Martín Pendás, A.; Blanco, M. A. *J. Chem. Phys.* **2007**, *126*, 094102.
(41) Martín Pendás, A.; Francisco, E.; Blanco, M. A *J. Chem. Phys.* **2007**, *127*, 144103.
(42) Martín Pendás, A.; Francisco, E.; Blanco, M. A. *Phys. Chem. Chem. Phys.* **2007**, *9*, 1087.
(43) Yamasaki, T.; Goddard, W. A., III. *J. Phys. Chem. A* **1998**, *102*, 2919.
(44) Yamasaki, T.; Mainz, D. T.; Goddard, W. A., III. *J. Phys. Chem. A* **2000**, *104*, 2221.
(45) Martín Pendás, A.; Francisco, E.; Blanco, M. A. *Faraday Discuss.* **2007**, *135*, 423.
(46) Schmidt, M. W.; Baldridge, K. K.; Boatz, J. A.; Elbert, S. T.; Gordon, M. S.; Jensen, J. H.; Koseki, S.; Matsunaga, N.; Nguyen, K. A.; Su, S. J.; Windus, T. L.; Dupuis, M.; Montgomery, J. A. *J. Comput. Chem.* **1993**, *14*, 1347.
(47) Martín Pendás, A.; Francisco, E.; Blanco, M. A. *Chem. Phys. Lett.* **2007**, *437*, 287.
(48) Garcia-Revilla, M.; Hernandez-Trujillo, J. *Phys. Chem. Chem. Phys.* **2009**, *11*, 8425.
(49) Delchev, V. B.; Nikolov, G. S. *Monatsh. Chem.* **2000**, *131*, 99.
(50) Weinhold, F.; Landis, C. *Valency and Bonding. A Natural Bond Orbital Donor-Acceptor Perspective*; Cambridge Univ. Press: Cambridge, U.K., 2005.